

# Prospective Identification of CRT Super Responders Using a Motion Atlas and Random Projection Ensemble Learning

Devis Peressutti<sup>1</sup>, Wenjia Bai<sup>2</sup>, Thomas Jackson<sup>1</sup>, Manav Sohal<sup>1</sup>, Aldo Rinaldi<sup>1</sup>, Daniel Rueckert<sup>2</sup>, and Andrew King<sup>1</sup>

<sup>1</sup> Division of Imaging Sciences & Biomedical Engineering, King's College London, UK

<sup>2</sup> Biomedical Image Analysis Group, Imperial College London, UK

**Abstract.** Cardiac Resynchronisation Therapy (CRT) treats patients with heart failure and electrical dyssynchrony. However, many patients do not respond to therapy. We propose a novel framework for the prospective characterisation of CRT 'super-responders' based on motion analysis of the Left Ventricle (LV). A spatio-temporal motion atlas for the comparison of the LV motions of different subjects is built using cardiac MR imaging. Patients likely to present a super-response to the therapy are identified using a novel ensemble learning classification method based on random projections of the motion data. Preliminary results on a cohort of 23 patients show a sensitivity and specificity of 70% and 85%.

## 1 Introduction

Cardiac resynchronisation therapy (CRT) has the potential to improve both morbidity and mortality in selected heart failure patients with electrical dyssynchrony. Standard selection criteria for CRT are a New York Heart Association functional class of II to IV, a QRS duration  $> 120ms$ , and a Left Ventricular (LV) ejection fraction (EF)  $\leq 35\%$ . However, when applying such criteria, a large variability in the response rate has been reported [1]. Improved characterisation of patients likely to respond to the treatment is therefore of clinical interest.

In recent years, there has been a growing interest in the characterisation of CRT *super-response*. Super-responders exhibit an enhanced level of LV Reverse Remodelling (RR) after CRT, which leads to an almost complete recovery of cardiac function [2]. Recent studies have shown strong evidence for super-response in patients with strict left bundle branch block (LBBB) [11] and a type II electrical activation pattern (also known as U-shaped activation) [8]. A strict LBBB is characterised by a longer QRS duration ( $\geq 140ms$  in men and  $\geq 130ms$  in women) and a mid-QRS notching, while a U-shaped activation pattern is typically characterised by a line of functional block located between the septum and the lateral wall and by a delayed trans-septal conduction time [8].

However, characterisation of the complex LV electrical activation based only on strict LBBB and a U-shaped activation pattern, although promising, is rather

simplistic. As noted in [8], assessment of contraction patterns is a subjective process and it is possible that such a classification might fail to capture the complex variation in electrical and mechanical activation patterns. Assuming a coupled electrical and mechanical LV activation, we propose a more sophisticated characterisation of LV contraction for the prediction of CRT super-response. Using Cardiac Magnetic Resonance (CMR) imaging, the LV mechanical contraction of a population of CRT patients is estimated and a spatio-temporal LV motion atlas is built, allowing direct comparison of LV contractions of different patients. Random projection ensemble learning is used to prospectively identify super-responders based on the LV contraction information only. Previous related work includes [5,4], where a LV motion atlas was used to identify specific abnormal activation patterns, such as Septal Flash. However, to the authors' knowledge, this is the first work seeking to characterise CRT super-responders using machine learning on 3D motion descriptors.

## 2 Materials

A cohort of 23 patients<sup>1</sup> fulfilling the conventional criteria for CRT (see Sect. 1) was considered. The study was approved by the institutional ethics committee and all patients gave written informed consent. All patients underwent CMR imaging using a 1.5T scanner (Achieva, Philips Healthcare, Best, Netherlands) with a 32-element cardiac coil. The acquired CMR sequences are as follows:

**cine MR:** A multi-slice SA and three single-slice LA (2, 3 and 4-chamber view) 2D cine Steady State Free Precession (SSFP) sequences were acquired (TR/TE = 3.0/1.5ms, flip angle = 60°). Typical slice thickness is of 8mm for SA and 10mm for LA with an in-plane resolution  $\approx 1.4 \times 1.4\text{mm}^2$ ;

**T-MR:** Tagged MR sequences in three orthogonal directions with reduced field-of-view enclosing the left ventricle were acquired (TR/TE = 7.0/3.2ms, flip angle = 19 – 25°, tag distance = 7mm). The typical spatial resolution in the plane orthogonal to the tagging direction is  $\approx 1.0 \times 1.0\text{mm}^2$ ;

All images were ECG-gated and acquired during sequential breath-holds. Given their high in-plane spatial resolution, the cine MR images at end-diastole (ED) were employed to estimate LV geometry (see Sect. 3.1), while the cine MR images at the other cardiac phases were not used in this work. An average high resolution  $3D + t$  T-MR sequence was derived from the three T-MR acquisitions with orthogonal tagging directions and was used to estimate the LV contraction (see Sect. 3.1). Prior to the estimation of LV geometry and motion, the SA and LA cine MR sequences were spatially aligned to the T-MR coordinate system. Such spatial alignment compensates for motion occurring between sequential breath-holds. The T-MR sequence is free from respiratory artefacts and therefore was chosen as the reference coordinate system.

Different super-response measures that quantify the degree of RR have been proposed [2,11]. In this work, we employ a combined measure of super-response,

---

<sup>1</sup> Data were acquired from different projects and cannot be made publicly available due to lack of ethical approval or patient consent on data sharing.

characterised by a LV end-diastolic volume reduction  $\leq 20\%$ , a LV end-systolic volume reduction  $\leq 15\%$  and a two-fold increase in LV ejection fraction or an absolute value  $\geq 40\%$ . According to this classification, 10 out of 23 patients in our cohort were classified as super-responders. This binary classification was used to train the proposed ensemble learning classifier (see Sect. 3.2).

### 3 Methods

The main novelty of the proposed method lies in the application of a novel dimensionality reduction technique for the characterisation of CRT super-response. The proposed framework is summarised in Fig. 1.

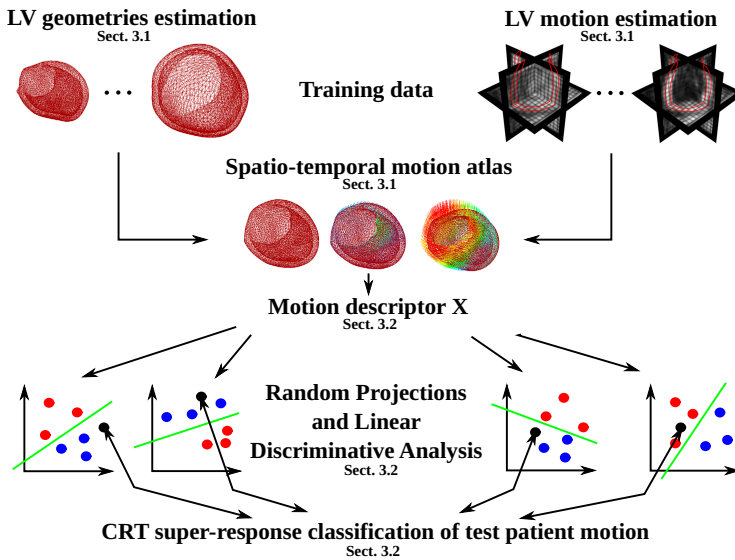


Fig. 1. Overview of the proposed framework.

Similarly to [4], a spatio-temporal motion atlas of the LV was built to allow motion comparison from different patients. The atlas removes differences in LV anatomy and cardiac cycle duration from the comparison of LV motion. Details of the atlas formation are reported in Sect. 3.1, while Sect. 3.2 describes the random projection ensemble classifier used to characterise super-responders.

#### 3.1 Spatio-Temporal Motion Atlas

The LV spatio-temporal motion atlas formation comprises the following steps:

**Estimation of LV Geometry.** For each patient, the LV myocardium, excluding papillary muscles, was manually segmented from the ED frames of the multi-slice SA and three LA cine MR images and the four binary masks were fused together into an isotropic  $2mm^3$  binary image. Following a further manual refinement of

the binary mask to obtain a smooth LV segmentation, an open-source statistical shape model (SSM) of the LV [7] was employed to enforce point correspondence amongst all LV geometries. After an initial landmark-based rigid alignment, the SSM was optimised to fit the LV segmentation. Non-rigid registration followed the mode optimisation to refine local alignment. An example of a LV surface is shown in Fig. 2(a)-(e).

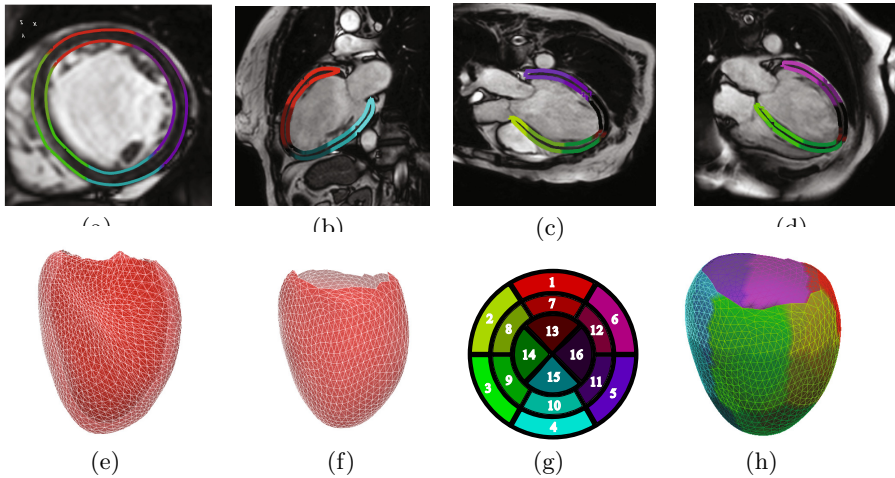


**Fig. 2.** Example of estimated LV geometry at end-diastole overlaid onto (a) mid SA slice, (b) 2-, (c) 3-, and (d) 4-chamber cine LA slices. Fig. (e) shows the resulting SSM epi- and endo-cardial meshes, while (f) shows the resampled medial mesh. Fig. (g) shows the AHA bull's eye plot, while (h) shows the unbiased medial shape.

In order to spatially regularise the number of vertices, a medial surface mesh with regularly sampled vertices ( $\approx 1500$ ) was generated from the personalised SSM epi- and endo-cardial surfaces (Fig. 2(f)). The same resampling strategy was employed for all patients to maintain point correspondence.

**Estimation of LV Motion.** An average high resolution  $3D+t$  T-MR sequence was derived from the  $3D+t$  T-MR sequences with orthogonal tagging planes. For each T-MR volume, the trigger time  $t_T$  specified in the DICOM meta-tag was normalised with respect to the patient's average cardiac cycle, such that  $t_T \in [0, 1)$ , with 0 being ED. LV motion with respect to the ED cardiac phase was estimated using a  $3D+t$  free-form-deformation algorithm with sparse spatial and temporal constraints [10]. This algorithm estimates a smooth and continuous  $3D+t$  transformation for any  $t \in [0, 1)$ . This way, temporal normalisation was achieved for each patient, regardless of the number of acquired T-MR volumes and cycle length.

**Spatial Normalisation.** The aim of spatial normalisation is to remove bias towards patient-specific LV geometries from the motion analysis. From the previous steps, LV shapes at ED (see Fig. 2(f)) were derived from  $N$  patients.

An initial Procrustes alignment based on the point correspondences was performed on the  $N$  medial LV shapes, obtaining a set of affine transformations  $\{\phi_{aff}^n\}, n = 1, \dots, N$  with respect to a randomly chosen reference shape. An unbiased LV medial shape was computed by transforming the average shape of the aligned surfaces by the inverse of the average affine transformation  $\tilde{\phi}_{aff} = \frac{1}{n} \sum_n \phi_{aff}^n$ . An example of an unbiased LV shape is shown in Fig. 2(h). In order to enforce an identity average transformation, the original transformations  $\{\phi_{aff}^n\}$  were similarly normalised  $\hat{\phi}_{aff}^n = \phi_{aff}^n \circ (\tilde{\phi}_{aff})^{-1}$ . All shapes were consequently aligned to the unbiased medial LV shape using Thin Plate Spline (TPS) transformations  $\{\phi_{TPS}^n\}$ . The transformation from the patient-specific coordinate system to the unbiased LV mesh is thus given by  $\phi^n = \phi_{TPS}^n \circ \hat{\phi}_{aff}^n$  [4].

**Motion Reorientation.** In order to compare cardiac phases amongst all patients, for each patient, the reference ED medial surface was warped to  $T = 24$  cardiac phases equally distributed in  $[0, 0.8]$  by using the estimated  $3D+t$  transformation. Only the first 80% of the cardiac cycle was considered since it represents the typical coverage of T-MR sequences, and the estimated motion for  $t \in (0.8, 1]$  is due to interpolation. The patient-specific LV motion was therefore fully represented by the  $T$  shapes. Under a small deformation assumption [4],  $\mathbf{v}_{p,t}^n = \mathbf{u}_{p,t}^n - \mathbf{u}_{p,0}^n$  denotes the motion at location  $\mathbf{u}$  of vertex  $p \in 1, \dots, P$  at the cardiac phase  $t \in 1, \dots, T$  with respect to the ED phase for patient  $n \in 1, \dots, N$ . The patient-specific motion  $\mathbf{v}_{p,t}^n, \forall n, t, p$  is transported to the coordinate system of the unbiased average shape by computing  $\mathbf{v}_{n,p,t}^{atlas} = J^{-1}(\phi^n(\mathbf{u}_p)) \cdot \mathbf{v}_{p,t}^n$ , where  $J(\phi^n)$  denotes the Jacobian of the transformation  $\phi^n$  [4].

**AHA Segmentation.** For a more intuitive understanding of the LV motion, the atlas was segmented into the standard 16 AHA segments [3] (see Fig. 2(g) and 2(h)) and the LV motion  $\mathbf{v}_{n,p,t}^{atlas}$  was decomposed into longitudinal, radial and circumferential cylindrical coordinates ( $\mathbf{v}_{n,p,t}^{atlas} = [l_{n,p,t}, r_{n,p,t}, c_{n,p,t}]^T$ ) with respect to the long axis of the LV ED medial surface.

### 3.2 Random Projection Ensemble Learning

The spatio-temporal atlas permits representation of the LV motion in a common coordinate system  $\mathbf{v}_{n,p,t}^{atlas}, \forall n, p, t$ . For each patient  $n$ , a LV motion descriptor was derived by concatenating  $\mathbf{v}_{p,t}^{atlas}, \forall p, t$  into a single column vector  $\mathbf{v}_n \in \mathbb{R}^F$ , where  $F$  denotes the number of features of the motion descriptor. After normalisation,  $\tilde{\mathbf{v}}_n = \frac{\mathbf{v}_n}{\|\mathbf{v}_n\|}$ , the training data set was given by  $\mathbf{X} = [\tilde{\mathbf{v}}_1 \cdots \tilde{\mathbf{v}}_N] \in \mathbb{R}^{F \times N}$ . The aim of the proposed technique is to find a set of low-dimensional representations of the high dimensional motion matrix  $\mathbf{X}$  that maximises super-response classification.

Typical limitations in the analysis of high dimensional data are the presence of noisy features and the curse of dimensionality (i.e. data is very sparse in a high dimensional space). These factors can hinder the identification of the underlying structure of the data. To overcome these limitations, linear and non-linear dimensionality reduction techniques have been proposed to transform the original high dimensional data onto lower dimensional subspaces, where the underlying

data structure is described according to some criteria. For instance, Principal Component Analysis (PCA) projects the original data onto a linear subspace that preserves the variance of the data. However, the resulting subspace might not be optimal for the classification task at hand.

A novel ensemble learning classifier employing Random Projections (RPs) has been recently proposed in [6]. In our work, we extend [6] by using RPs and Linear Discriminant Analysis (LDA) to identify an optimal set of subspaces that best performs on the given classification. Let  $\mathbf{Y} \in \mathbb{R}^N$ ,  $y_n \in \{0, 1\}$  be the CRT super-response labels (0-no super-response, 1-super-response, see Sect. 2 for the classification criteria),  $L$  the number of classifiers in the ensemble and  $D$  the number of dimensions of the random subspace ( $D \ll F$ ). In the training phase, for each classifier  $C_l$ ,  $l = 1, \dots, L$ , the motion matrix  $\mathbf{X}$  was projected onto a random subspace defined by a sparse random matrix  $\mathbf{R}_l \in \mathbb{R}^{D \times F}$ , in which the elements of each column vector  $\{r_i\}_{i=1}^F$  are drawn from a Bernoulli  $\{+1, -1\}$  distribution with  $\|r_i\| = 1$ . As a result of the random projection, a new set of low-dimensional descriptors  $\mathbf{Z} = \mathbf{R} \cdot \mathbf{X}$ ,  $\mathbf{Z} \in \mathbb{R}^{D \times N}$  was generated and a LDA classifier was trained on the descriptors  $\mathbf{Z}$  and the class labels  $\mathbf{Y}$ .

In this work we extend [6] to improve the robustness of the random subspace generation, as follows. The performance of each classifier was evaluated on the same training data and the number of misclassified patients  $M$  was computed. If the misclassification was larger than a predefined percentage  $M > k \cdot N$ ,  $\mathbf{R}$  was discarded and a new random projection was generated. This process was repeated for each classifier  $C_l$  until an acceptable projection  $\mathbf{R}_l$  was found. As a consequence, the random subspace selection is more robust, even with a low number of classifiers. The value of  $k$  defines the accuracy of the selected subspace. Low values of  $k$  generate very discriminative subspaces at the cost of a higher computational time (a maximum number of iterations can also be introduced).

The result was a set of linear classifiers trained on RPs of the motion matrix  $\mathbf{X}$  which are highly discriminative with respect to CRT super-response. In the testing phase, the motion vector of a test patient  $\mathbf{x}_{test} \in \mathbb{R}^F$  was projected onto the selected random subspaces  $\{\mathbf{R}_l\}_{l=1}^L$  and the CRT super-response class was predicted by the  $L$  trained LDA classifiers. The final super-response class  $y_{test}$  was derived by a weighted average of the  $L$  predicted classes  $\{y_{test_l}\}_{l=1}^L$ , where the weight for each classifier  $C_l$  is given by the residual misclassification error  $M$  (the higher the residual misclassification error  $M$ , the lower the weight) [9]. The super-response class with highest cumulative weights was assigned to  $y_{test}$ .

## 4 Experiments and Results

To evaluate the proposed technique, a leave-one-out cross-validation was employed. Each patient was left-out in turn and the motion descriptor  $\mathbf{X}$  was built using the remaining  $N = 22$  patients. The LV motion of the left-out patient constituted the test motion descriptor  $\mathbf{x}_{test}$ .

Since both strict LBBB and U-shaped activation are related to localised activation patterns [8], we investigated the influence of different LV regions on the super-response classification. Three different motion descriptors  $\mathbf{X}_{16}$ ,  $\mathbf{X}_6$  and

$\mathbf{X}_3$  were built considering a different number of AHA segments as follows.  $\mathbf{X}_{16}$  was built considering all the vertices in the atlas ( $F \approx 110,000$ ),  $\mathbf{X}_6$  was built considering the six AHA segments 7 – 12 in the mid LV ( $F \approx 38,000$ ) and  $\mathbf{X}_3$  was built considering only the three AHA segments 7, 8, 12 ( $F \approx 17,000$ ) located in proximity to the conduction block line [8] (see Fig. 2(g)).

The proposed technique ( $RLDA_{wr}$ ) was compared to a LDA classification applied to the high dimensional motion matrices ( $LDA$ ), a LDA classification applied to a low-dimensional subspace given by PCA ( $PLDA$ ), and to the RPs ensemble classifier with no subspace rejection ( $RLDA$ ) [6]. For the  $PLDA$  technique, a dual formulation was employed since  $N \ll F$ , and the modes retaining 95% of the original variance were considered. A super-response classification based on the presence of strict LBBB only is also reported for comparison. The set of parameters used for  $RLDA_{wr}$  was determined from an initial pilot study using the same training data (see Table 1). The same parameters  $L, D$  were employed for  $RLDA$ , while the value of  $k$  was fixed  $k = 0.1$ .

Results of the leave-one-out cross-validation are reported in Table 1.

**Table 1.** Cross-validation results for sensitivity, specificity, positive (PPV) and negative predictive value (NPV). The subspace dimensionality  $D$  and, where applicable, the number of classifiers  $L$  is also reported. Best classification results are shown in bold.

	$\mathbf{X}_{16}$				$\mathbf{X}_6$				$\mathbf{X}_3$				LBBB
	$LDA$	$PLDA$	$RLDA$	$RLDA_{wr}$	$LDA$	$PLDA$	$RLDA$	$RLDA_{wr}$	$LDA$	$PLDA$	$RLDA$	$RLDA_{wr}$	
Sens	.40	.70	.50	.60	.40	.50	.40	.50	.50	.60	.60	<b>.70</b>	.80
Spec	.62	.62	.62	.69	.62	.69	.77	.85	.77	.61	.77	<b>.85</b>	.62
PPV	.44	.58	.50	.60	.44	.55	.57	.71	.63	.55	.66	<b>.78</b>	.62
NPV	.57	.72	.62	.69	.57	.64	.63	.69	.67	.67	.71	<b>.79</b>	.80
$D$	$F$	17	20	20	$F$	15	30	30	$F$	13	200	200	NA
$L$	NA	NA	61	61	NA	NA	61	61	NA	NA	61	61	NA

## 5 Discussion

We have presented a method for the automatic prospective identification of CRT super-responders based purely on motion information estimated from CMR imaging. The novelty of this paper lies in the application and extension of a recently proposed dimensionality reduction algorithm to a clinically important, but previously untackled problem in medical image processing. Our extension to the random projections ensemble learning technique [6] consists of a more robust selection of the random subspace with respect to the classification accuracy.

Results on a cohort of 23 CRT patients show the proposed technique  $RLDA_{wr}$  to outperform  $PLDA$  and  $RLDA$  in the selection of an optimal subspace for classification of CRT super-responders. The best classification results were achieved considering only three AHA segments localised around the conduction block line, which supports the findings in [8] on the correlation between the presence of a U-shaped contraction and super-response. Compared to a LBBB-based classification [11] (last column in Table 1), better specificity and PPV were achieved.

In the future, we plan to expand our patient cohort to enable our algorithm to learn a wider range of motion-based biomarkers that are correlated with CRT super-response. Much work remains to be done to better understand CRT response and super-response. At the moment, relatively simple indicators are used to select patients for CRT and many that undergo the invasive therapy do not respond. Furthermore, there is currently no consensus on the definition of a super-responder. It may be that a better characterisation of LV mechanical activation patterns could lead to a more functional definition of super-response. Our method offers the possibility of providing insights into these motion patterns, which could lead to a more refined characterisation of LV function than is currently possible. We have demonstrated our technique on the problem of identifying super-responders, but we believe that it could one day complement or even replace conventional indicators for predicting CRT response in general.

**Acknowledgements.** This work was funded by EPSRC Grants EP/K030310/1 and EP/K030523/1. We acknowledge financial support from the Department of Health via the NIHR comprehensive Biomedical Research Centre award to Guy's & St Thomas' NHS Foundation Trust with KCL and King's College Hospital NHS Foundation Trust.

## References

1. Abraham, W.T., et al.: Cardiac resynchronization in chronic heart failure. *The New England Journal of Medicine* 346(24), 1845–1853 (2002)
2. António, N., et al.: Identification of 'super-responders' to cardiac resynchronization therapy: the importance of symptom duration and left ventricular geometry. *Europace* 11(3), 343–349 (2009)
3. Cerqueira, M.D., et al.: Standardized Myocardial Segmentation and Nomenclature for Tomographic Imaging of the Heart. *Circulation* 105(4), 539–542 (2002)
4. De Craene, M., et al.: SPM to the heart: Mapping of 4D continuous velocities for motion abnormality quantification. In: 2012 IEEE ISBI, pp. 454–457 (2012)
5. Duchateau, N., et al.: A spatiotemporal statistical atlas of motion for the quantification of abnormal myocardial tissue velocities. *Medical Image Analysis* 15(3), 316–328 (2011)
6. Durrant, R., et al.: Random projections as regularizers: learning a linear discriminant from fewer observations than dimensions. *Machine Learning*, 1–16 (2014)
7. Hoogendoorn, C., et al.: A High-Resolution Atlas and Statistical Model of the Human Heart From Multislice CT. *IEEE Transactions on Medical Imaging* 32(1), 28–44 (2013)
8. Jackson, T., et al.: A U-shaped type II contraction pattern in patients with strict left bundle branch block predicts super-response to cardiac resynchronization therapy. *Heart Rhythm* 11(10), 1790–1797 (2014)
9. Kim, H., et al.: A weight-adjusted voting algorithm for ensembles of classifiers. *Journal of the Korean Statistical Society* 40(4), 437–449 (2011)
10. Shi, W., et al.: Temporal sparse free-form deformations. *Medical Image Analysis* 17(7), 779–789 (2013)
11. Tian, Y., et al.: True complete left bundle branch block morphology strongly predicts good response to cardiac resynchronization therapy. *Europace* 15(10), 1499–1506 (2013)